Metallomics

Indexed in Medline!

ROYAL SOCIETY OF CHEMISTRY

PAPER
Carl J. Carrano *et al.*
Surface binding, localization and storage of iron in the giant kelp
Macrocystis pyrifera

Surface binding, localization and storage of iron in the giant kelp *Macrocystis pyrifera*

Eric P. Miller,[a] Hendrik Auerbach,[b] Volker Schünemann,[b] Teresa Tymon[a] and Carl J. Carrano*[a]

Iron is an essential element for all living organisms due to its ubiquitous role in redox and other enzymes, especially in the context of respiration and photosynthesis. Although the iron uptake and storage mechanisms of terrestrial/higher plants have been well-studied, the corresponding systems in marine algae have received far less attention. While the iron many marine algae take up from the environment, irrespective of its detailed internalization mechanism, arrives at the cell surface by diffusion, there is growing evidence for more "active" means of concentrating this element prior to uptake. It has been well established in both laboratory and environmentally derived samples, that a large amount of iron can be "non-specifically" adsorbed to the surface of marine algae. While this phenomenon is widely recognized and has prompted the development of experimental protocols to eliminate its contribution to iron uptake studies, its potential biological significance as a concentrated iron storage source for marine algae is only now being recognized. In this study, using an interdisciplinary array of techniques, we show that the giant kelp *Macrocystis pyrifera* also displays significant cell surface bound iron although less than that seen with the related brown alga *Ectocarpus siliculosus*. The iron on the surface is likely bound to carboxylate groups and once inside the iron is found to localize differently depending on cell type. Iron appears to be stored in an as yet undefined mineral phase.

Significance to metallomics

Understanding how iron, an essential element for all living organisms due to its ubiquitous role in redox and other enzymes, is taken up and stored by marine plant-like linages is important given that this element is often the growth limiting micronutrient. While many uptake and storage mechanisms are known and have been characterized, this study provides evidence that binding to the cell surface is of potential biological significance as a concentrated iron storage source for such organisms.

Introduction

Iron is an essential element for all living organisms due to its ubiquitous role in redox and other enzymes, especially in the context of respiration and photosynthesis. The iron uptake and storage systems of terrestrial/higher plants are now reasonably well understood with two basic strategies for iron uptake being distinguished: Strategy I plants, mainly dicotyledons, use a mechanism involving soil acidification and induction of Fe(III)-chelate reductase (ferrireductase) and Fe(II) transporter proteins.[1,2] Strategy II plants (in particular, monocotyledons/grasses) have evolved sophisticated systems, similar to those of bacteria and fungi, based on high-affinity, iron specific, binding compounds called phytosiderophores.[3]

In contrast, there is little knowledge about the corresponding systems in marine, plant-like lineages; particularly the multicellular macroalgae (seaweeds). This is important as the iron level in ocean waters is even lower than in most terrestrial environments due both to the low solubility of Fe(III) in oxic seawater and the fact that a large fraction of the limited iron available is already tightly complexed.[4] Indeed, iron availability is now well known to limit primary productivity in certain oceanic regimes.[5]

While it seems likely that the iron many marine algae take up from the environment, irrespective of its detailed internalization mechanism, arrives at the cell surface by diffusion, there is growing evidence for more "active" means of concentrating this

[a] *Department of Chemistry and Biochemistry, San Diego State University, San Diego, CA 92182-1030, USA. E-mail: ccarrano@mail.sdsu.edu*
[b] *Department of Physics, Technical University Kaiserslautern, 67663 Kaiserslautern, Germany*

element prior to uptake. It has been well established in both laboratory and environmentally derived samples, that a large amount of iron can be "non-specifically" adsorbed to the surface of marine algae.[6] This surface bound iron may derive from simple electrostatic attraction between colloidal iron hydroxide particles and the cell surface, from de novo precipitation of iron hydroxo polymers from equilibrium solutions at the cell surface due to the increased surface pH relative to bulk seawater, or other mechanisms.[7] While this surface adsorption phenomenon is widely recognized and has prompted the development of experimental protocols to eliminate its contribution to iron uptake studies, its potential exploitation as a concentrated iron source for marine algae is only now being recognized.[8,9] Recent examples of possible surface concentration of iron come from the diatoms, the Alveolate Chromera velia, and Ectocarpus siliculosus where in some cases there is evidence that the surface bound iron is ultimately internalized.[10–12]

While efficient transport mechanisms for iron uptake are an essential element in all pro- and eukaryotic cells, its intracellular availability and storage has to be tightly regulated, not only to buffer supply and demand, but also to prevent cell damage from undesirable reactions of free radicals, formed catalytically by free Fe ions. Ferritin represents the most common form of iron storage in all domains of life. This water-soluble protein is composed of a tetraeicosameric shell built up by polypeptide subunits and a microcrystalline core of ferrihydrite within the protein cavity. A general structural model of ferritins has been derived from X-ray diffraction studies.[13,14] Although the general topology of most ferritins is similar, a remarkable heterogeneity of the ferritin subunits is observed which is the basis of different classes of ferritins including various types of bacterial ferritins i.e. heme containing bacterioferritins (Bfr), non-heme bacterial ferritins Ftn1 and Ftn2, "miniferritins" (exhibiting a dodecahedral peptide assembly), and various animal and plant "maxiferritins". Numerous functions have been attributed to these ferritins. One function is associated with "true" iron storage. Under iron-rich growth conditions the metal is accumulated in order to provide an iron pool sufficiently high to prevent growth limitation effects in an iron-deficient environment. A second function is associated with the potentially harmful role iron can play in cell physiology by generating OH$^\bullet$ and other oxygen radicals (Haber–Weiss–Fenton reaction cycle).[15]

Brown algae (Phaeophyta) belong to a lineage that has been evolving independently of other major photosynthetic lineages, such as green plants (Chlorophyta) and red algae (Rhodophyta). Instead, they are classified within the Stramenopiles and Chromalveolates together with diatoms, golden-brown algae and oomycetes.[16] As a consequence of this singular evolutionary history, brown algae exhibit many unusual, and often unique, features. These features are adaptations to the marine coastal environments in which brown algae are usually the dominant organisms in terms of biomass, especially in terms of the extensive kelp forests. Along the west coast of North America, the primary canopy-forming kelp is the giant kelp, Macrocystis pyrifera, (hereafter Macrocystis) which dominates this ecosystem from the Pacific coast of central Baja California, México to central

California, USA, and parts of coastal Alaska., Macrocystis is also the dominant canopy forming kelp throughout much of the coastal ecosystems in the southern Hemisphere, including Peru, Chile, Argentina, South Africa, Australia, New Zealand and the Sub-Antarctic Islands, rendering it of global importance.

Taxonomically, Macrocystis belongs to the family Lessoniaceae, a group of kelps that are characterized by meristems that repeatedly split and often have gas-filled pneumatocysts that buoy the thallus at the sea surface. The thallus of Macrocystis is composed of three primary tissue types; holdfasts that anchor the kelp to the substrate, stipes that grow vertically towards the water surface, and blades that are the primary sites of photosynthesis. Blades and stipes are often collectively referred to as fronds, and comprise the majority of the three-dimensional structure in the water column. Within the stipe tissue, a series of elongated sieve cells occur within the outer cortex where they are aligned end-to-end and allow the transport of photosynthetic products (e.g. mannitol) from the blades (site of photosynthesis) downward toward the holdfast where new fronds are initiated. Transport in these cells can occur as rapidly as 65–78 cm h^{-1} and resembles phloem translocation in vascular plants.[17] With a length of up to around 60 m, Macrocystis is by far the largest seaweed in the world and, indeed, one of the largest organisms on Planet Earth. Further, due to its exceptionally large standing stock and growth rate (up to 30 cm per day linear growth, the highest of any living organism), Macrocystis is of paramount ecological and economic importance. It is the single largest source of raw material for the global alginate industry and supports an economic activity of several hundred million dollars annually. Herein we address the questions of surface binding, localization and storage of iron in the giant kelp Macrocystis pyrifera.

Methods

Algal culture

Macrocystis was harvested from the Point Loma kelp forest (32.7 N, 117.3 W) and either used immediately after collection or maintained in a photobioreactor (New Brunswick Scientific, USA) containing aerated Provasoli-enriched Scripps Pier sea water ($\sim$4 nM Fe) at 12 °C under a 14/10 light/dark photocycle. Ectocarpus siliculosus was grown and maintained as previously described.[12]

Titanium(III)–citrate–EDTA reagent

The titanium(III)–citrate–EDTA reagent was prepared according to Hudson and Morel to remove extracellular iron from Macrocystis.[9] Briefly, water was deoxygenated by boiling, allowed to cool under a stream of nitrogen gas, and the following solids were dissolved such that citrate [0.047 M], EDTA [0.047 M], NaCl [0.35 M], KCl [0.01 M]. The pH was adjusted to ca. 8 with NaOH and then 7.77 mL 20% aqueous $TiCl_3$ was added giving [0.047 M] Ti(III). The pH was again adjusted with NaOH dropwise to pH 8.1 and the final reagent was stored anaerobically in a drybox until further use. The Ti(III)–citrate–EDTA reagent was applied to the Macrocystis sample after rinsing with artificial seawater (ASW). 5 mL of the reagent was added to Macrocystis

and allowed to incubate for 2 min. It was removed by vacuum filtration followed by a 25 mL wash with ASW. Finally, *Macrocystis samples* were dried by vacuum filtration for subsequent scintillation counting. The resulting scintillation signal originates solely from internal ^{55}Fe.

Histochemistry

Ferrocyanide–diaminobenzidine (Perls–DAB) staining. *Macrocystis pyrifera* was harvested from the Point Loma kelp forest and blade discs were bored with a coring tool. Discs were fixed in a 0.1 M phosphate buffer solution containing 2% (w/v) paraformaldehyde, 1% (w/v) glutaraldehyde, and 1% (w/v) caffeine for 2 hours. The fixed cells were then washed with 0.1 M phosphate buffer and dehydrated in successive ethanol baths of 30%, 50%, 75%, 85%, 95%, and 100% (3×). The cells were then embedded in 1:1 (v/v) ethanol/LR White resin (EMS) for 3 hours followed by 100% LR White overnight in gelatin capsules under vacuum. Three micron sections were cut on a Leica EMUC6 microtome and deposited on glass slides. The Perls staining and DAB intensification procedure was performed as previously described.[18,19] Briefly, sections were incubated on glass slides with equal volumes 4% (v/v) HCl and 4% potassium ferrocyanide (Perls staining solution) for 45 minutes. After washing with distilled H_2O, sections were incubated in a methanol solution containing 0.01 M NaN_3 and 0.3% (v/v) H_2O_2 for 1 hour and then washed with 0.1 M phosphate buffer. DAB intensification was achieved by incubating sections in a 0.1 M phosphate buffer solution containing 0.00025–0.005% (w/v) DAB (Sigma), 0.005% (v/v) H_2O_2, and 0.005% (w/v) $CoCl_2$ for 30 minutes. The sections were then washed with H_2O before imaging with a Zeiss Axiovert 40 inverted microscope.

7-(4-Methylpiperazin-1-yl)-4-nitrobenzo-2-oxa-1,3-diazole (MPNBD) staining. *Macrocystis pyrifera* was harvested from the Point Loma kelp forest either by SCUBA (at depth) or small boat (surface) and kept on ice-cold seawater until it was returned to the lab. Samples were then subsequently embedded and cryofixed in Tissue-Tek® O.C.T. Compound (Electron Microscopy Sciences, USA) at liquid nitrogen temperature with a Leica CM1950 cryostat. Sections (50 µm thickness) were placed on glass well slides and allowed to thaw and then incubated for 5 minutes with a 0.025% working solution of MPNBD in methanol followed by three washes with 0.1 M phosphate buffer (pH 8.1). Wells were then mounted with coverslips and immediately viewed with a Nikon Eclipse TE2000-U inverted microscope (Nikon Imaging, Inc., Japan). MPNBD was prepared as described by Park.[20]

Energy-dispersive X-ray spectroscopy (EDS). *Macrocystis* fronds were harvested as described above and blade discs were cut with a coring tool and fixed in a pH 8.1, 0.1 M phosphate buffer solution containing 2% (w/v) paraformaldehyde, 1% (w/v) glutaraldehyde, and 1% (w/v) caffeine for 2 h. The fixed cells were then washed with 0.1 M phosphate buffer and dehydrated in successive ethanol baths of 30, 50, 75, 85, 95, and (3×) 100%. The cells were then embedded in 1:1 (v/v) ethanol/LR White resin (Electron Microscopy Sciences, USA) for 3 h followed by 100% LWR overnight in gelatin capsules under vacuum. Sections of 3 µm thickness were cut on a Leica EMUC6 microtome and

deposited on glass slides. Slides were coated with carbon in a Quorum Technologies Q150T ES sputter coater. Platinum-coated samples were analyzed under high vacuum in a Quanta 450 FEG environmental scanning electron microscope (ESEM) equipped with an Oxford Instruments INCA energy dispersive X-ray (EDX) microanalysis system.

Time-dependent and age-dependent surface binding studies. *Macrocystis* blade and stipe portions were transferred from a photobioreactor (New Brunswick Scientific, USA) to 250 mL culture flasks (Greiner, Germany) containing 10 µM radiolabeled $^{55/56}FeEDTA$ (Perkin-Elmer, USA) Provasoli enriched SPSW with $^{56}Fe:^{55}Fe$ ratio of 48:1. Blade and stipe samples were harvested after 4, 8, and 24 hours for the time-dependent study. Immature and mature blade and stipe samples were harvested after 24 hours for the age-dependent study. *Macrocystis* blade discs and stipe segments were washed with 25 mL ASW, and placed into pre-weighed scintillation vials (Millipore, USA) containing 1 mL of sodium hypochlorite (Fisher Scientific, USA). Vials were then weighed and subtracted to obtain *Macrocystis* mass. Samples were heated at 55 °C for 1 h to eliminate quenching effects originating from chlorophyll. 15 mL Hionic Fluor™ scintillation fluid (Perkin-Elmer, USA) was added to each scintillation vial and allowed to dark-adapt for at least 2 h in the scintillation counter (Beckman-Coulter LS 6500, USA) to eliminate any background chemiluminescence and phosphorescence prior to counting. Total iron uptake per mg dry *Macrocystis* cells was calculated based on specific activity, measured count rates, scintillation counting efficiency, and biomass measurements. Surface-bound iron was defined as the ^{55}Fe signal of cells not treated with Ti(III)–citrate–EDTA less the internalized iron signal of titanium washed replicates. Control data corresponding to internalized iron was defined as the ^{55}Fe signal of cells treated with Ti(III)–citrate–EDTA.

Enzymatic digestion of alginate in *Macrocystis* blade. Small sections of fresh blade tissue were cut and placed in Petri dishes containing 20 mL Provasoli enriched Scripps Pier sea water (SPSW) and 1 mg mL^{-1} alginate lyase (Sigma-Aldrich, USA). The Petri dish was covered to prevent evaporation and placed on a shaker inside an incubator maintained at 12 °C for 24 hours. The medium was then inoculated with radiolabeled $^{55/56}FeEDTA$ and allowed to incubate for an additional 24 hours. *Macrocystis* blade discs were harvested, washed with 25 mL ASW, and counted as described above.

EDTA-cell surface binding competition. An EDTA-cell surface chelate experiment was undertaken by preparing four ^{55}Fe radio-labeled Fe-EDTA stock solutions by adding $^{55}FeCl_3$ (1522 MBq mL^{-1}; Perkin-Elmer) to four ^{56}Fe-EDTA solutions (1:1.1, 1:10, 1:150 Fe:EDTA) such that $^{55}Fe:^{56}Fe$ equaled *ca.* 1:48. The stock solutions were allowed to equilibrate for at least 24 h prior to use. Six *Macrocystis* cultures with pH adjusted Scripps Pier sea water (∼4 nM Fe) media (3 at pH 4.0, 3 at pH 8.1) were inoculated with the ^{55}Fe-EDTA solutions to give a final [Fe] of 1 µM. *Macrocystis* was harvested, washed with 25 mL ASW, and placed into pre-weighed scintillation vials (Millipore, USA) containing 1 mL of sodium hypochlorite (Fisher Scientific, USA). Vials were then weighed and subtracted to obtain *Macrocystis* mass. Samples were heated at 55 °C for 1 h and 15 mL Hionic Fluor™

scintillation fluid (Perkin-Elmer, USA) added to each vial which was then allowed to dark-adapt for at least 2 h in the scintillation counter (Beckman-Coulter LS 6500, USA). Total iron uptake per mg dry *Macrocystis* cells was calculated based on specific activity, measured count rates, scintillation counting efficiency, and biomass measurements. Surface-bound iron was defined as the ^{55}Fe signal of cells not treated with Ti(III)–citrate–EDTA less the internalized iron signal of titanium washed replicates. Control data corresponding to internalized iron was defined as the ^{55}Fe signal of cells treated with Ti(III)–citrate–EDTA. Data was analyzed as described by Miller *et al.*[12]

Transmission Mössbauer spectroscopy (TMS). For cell surface binding studies *Macrocystis* fronds were harvested from the Point Loma kelp forest and then cultured in for 1 week in oligotrophic open ocean Pacific sea water (≈ 0.4 nM Fe) to remove adventitious ^{56}Fe from the cell surface. Blades were then transferred to 3 μM ^{57}Fe-EDTA enriched Scripps Pier sea water (SPSW) for 19 days. They were then harvested, either washed or not washed with Ti(III)–citrate–EDTA reagent, rinsed thoroughly with SPSW, packed into Delrin® Mössbauer sample holders and weighed. The Mössbauer spectra were recorded in the horizontal transmission geometry using a constant acceleration spectrometer operated in conjunction with a 512-channel analyzer in the time-scale mode (WissEl GmbH). The detector consisted of a proportional counter and the source consisted of 1.4 GBq [^{57}Co] diffused in Rh and was at room temperature. The spectrometer was calibrated against α-iron at room temperature (RT). For measurements at 77 K, samples were placed in a continuous-flow cryostat (Oxford Instruments). Spectral data were transferred from the multi-channel analyzer to a PC for further analysis employing the public domain program Vinda running on an Excel 2003® platform. Isomer shift δ, quadrupole splitting ΔE_Q, line width Γ and percentage of the total absorption area were obtained by least-squares fits of Lorentzian lines to the experimental spectra. All values are rounded to the last given digit. The isomers shifts, the quadrupole splitting and the line width are given in mms^{-1}. The relative area is given in parts per hundreds.

Results

Kinetics and thermodynamics of surface-bound iron

Fig. 1 shows the amount of radiolabeled iron retained after incubation with ^{55}Fe-EDTA for various times before washing with the Ti–citrate–EDTA reagent for both *Ectocarpus* and *Macrocystis*. While it is clear that *Ectocarpus* binds far more iron at the surface than does *Macrocystis*, it is equally evident that the latter also displays significant surface iron binding. This is made more evident in Fig. 2 which indicates that the amount of surface binding of iron (*i.e.* before washing with the Ti–citrate–EDTA reagent) to both mature and immature blades is some 10 times larger than the amount of iron internalized (*i.e.* after washing with Ti reagent). In addition it can be seen that immature *Macrocystis* blades (<1 m from frond apex) bind 7-fold more iron on the cell surface than that of mature blades (>3 m from apex). Immature blades also took up 40-fold more iron intracellularly than mature blades.
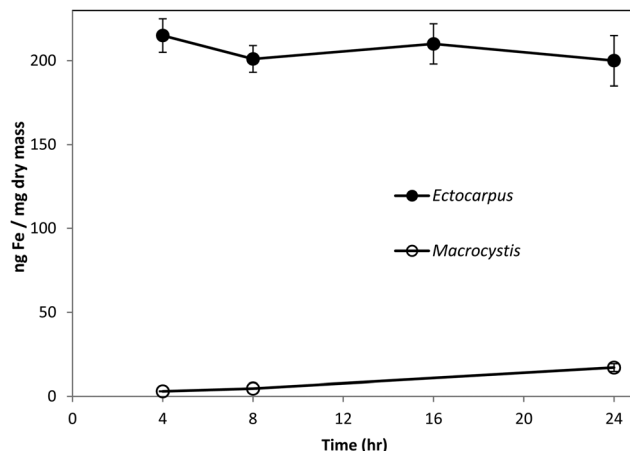

Fig. 1 Surface-binding of iron in *Ectocarpus* (closed circles) and immature *Macrocystis* blade (open circles) as a function of time. Error bars represent ±1 SD from triplicate measurements. Conditions as described in the text.

Macrocystis stipe exhibits a variable degree of cell surface iron binding depending on life-cycle. Immature stipe binds roughly twice as much iron on the cell surface than mature stipe, but significantly less than blade. In terms of intracellular iron, stipe age appears to have no effect. However, it is known that iron is concentrated in stipe sieve tube exudate (sieve sap) to a level 150-fold relative to seawater.[21] A variety of nutrients are assimilated in the blade and transported *via* the stipe through the water column to compensate for depth-dependent scarcities of nutrients and photons. Furthermore, potential iron chelators such as malate, phosphate, aspartate, and glutamate are common constituents of kelp sieve sap and are thus candidates for the stabilization of iron for long-distance translocation.[22] Therefore, whether this is true "uptake" as opposed to translocation of iron originating from the blade is unclear.

Our previous results with *Ectocarpus* suggested that alginate was the primary iron binding ligand in the cell wall.[12] This polysaccharide constitutes approximately 30–40% of the dry mass in both *Macrocystis* and *Ectocarpus*.[26,27] Carboxylates are moderately strong iron ligands, depending on the bonding mode. To determine if iron complexation at the cell wall in blades was
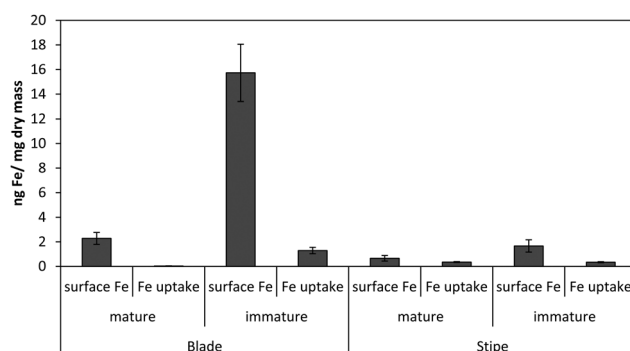

Fig. 2 Surface-bound *vs.* intracellular iron in *Macrocystis* blade and stipe as a function of life cycle after 24 hr incubation with ^{55}Fe. Other conditions as described in the text. Error bars represent ±1 SD from triplicate measurements.
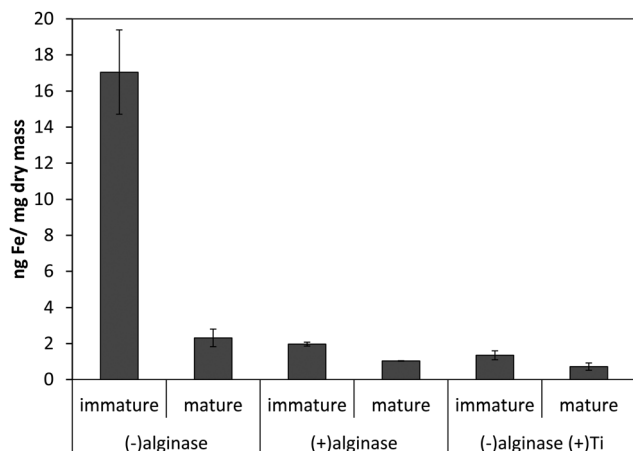
Fig. 3 Effect of 24 hour enzymatic digestion of *Macrocystis* blade as a function of life cycle. Other conditions as described in the text. Error bars represent ±1 SD from triplicate measurements.

Fig. 4 Immature *Macrocystis* blade cell surface binding of iron as a function of excess EDTA in growth medium. Error bars represent ±1 SD from triplicate measurements.

due to the presence of the carboxylate groups from alginate, alginate lyase (alginase) enzymatic digestion was performed on blade tissue. The magnitude of cell surface iron-binding after a 24 hour alginase incubation can be seen in Fig. 3. These results indicate that 96% of surface-bound iron is alginate-associated in immature blades while approximately 80% of surface-bound iron is alginate-associated in mature blades.

Although it was found that the high level of surface binding persisted with *Ectocarpus* until the EDTA to Fe concentration approached 100 : 1, *Macrocystis* retained only 30% of the surface-bound iron when the EDTA to Fe concentration approached 10 : 1 (Fig. 4) suggesting weaker surface binding of iron in the latter. However there is still significant surface-bound iron that must be complexed by high affinity ligands which out-compete EDTA even when the EDTA to Fe concentration approached 150 : 1 at physiological pH.

Measuring the surface binding from a solution of fixed [^{55}Fe] (1 μM) as a function of [EDTA] and pH allowed us to estimate an effective surface binding constant K_{eff}' as previously described.[12] The values obtained were relatively constant ($K_{eff}' = 10^{18}$ M^{-1}) over a wide range (0.1–1490 μM) of excess EDTA, confirming a uniform binding and the reliability of the data set. At high pH (8.1), iron binding is very strong (log $K_{eff}' = 18$) while at acidic pH (4.0) the binding constant is drastically reduced (log $K_{eff}' = 12$) presumably due to protonation of the alginate carboxylate groups thought to be the major iron binding moieties. The lower value of K_{eff}' relative to *Ectocarpus* may be due to differences in tissue architecture and/or the presence of a fucoidan mucous layer on *Macrocystis* blade surfaces. Fucoidan is a sulfated polysaccharide with several oxygen ligands which could potentially modulate the bonding mode of the carboxylato ligands giving rise to a weaker iron complex. Alternatively, fucoidan may simply form a physical barrier preventing the iron in seawater from accessing the cell wall.

Localization of Iron on the surface

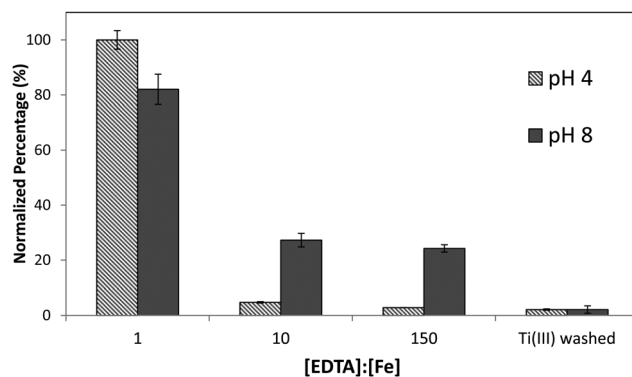Histochemical analyses were performed on environmental samples to investigate the spatial distribution and uniformity of iron bound to the cell surface using the ferrocyanide-3,3-diaminobenzidine (DAB) protocol. It is clear that the majority of the iron in samples not washed with the Ti(III) reagent is present on the surface with no internal iron visible in Ti(III) washed samples (Fig. 5).

While the ferrocyanide–DAB procedure was successful in visualizing extracellular iron in *Macrocystis*, the stain was ineffective for the visualization of internal iron stores. For this reason, the newly reported, highly sensitive, iron-specific, fluorescent probe MPNBD was synthesized and employed for both intra- and extracellular iron visualization in *Macrocystis*.[20] In *Macrocystis* blade, intense Fe-MPNBD fluorescence indicates iron concentrated to the meristoderm and to a lesser degree in the apoplast of the cortex (Fig. 6).

Likewise, in *Macrocystis* stipe iron is concentrated mostly to the meristoderm (Fig. 7). The stipe cortex appears to concentrate iron in the apoplast at a level slightly higher than that of blade cortex (Fig. 8).

This may be due to diffusion/leakage of iron from the medullar sieve cells where iron is concentrated to 150-fold the concentration of seawater.

As can be seen in Fig. 9, a significant amount iron is localized in the medulla. The large sieve cells appear to contain iron in the cell wall, sieve plate pores, and hyphae mitochondria.
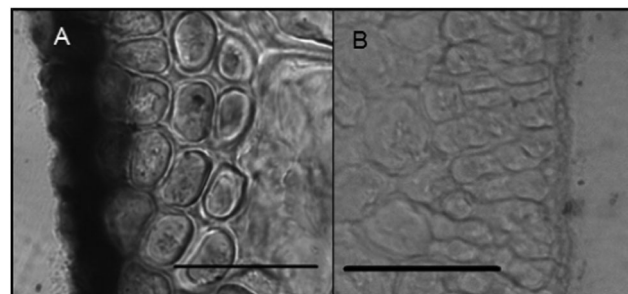

Fig. 5 DAB staining of environmental sample of immature *Macrocystis* blade. (A) Without Ti(III) wash, and (B) with Ti(III) wash. The black regions in (A) represent polyDAB catalyzed by high concentrations of extracellular iron. Scalebar, 20 μm.

We attempted to apply Energy Dispersive X-ray Spectroscopy (EDS) to confirm the localization of iron. However, the sensitivity of EDS was inadequate for the detection of iron in *Macrocystis* confirming the much reduced surface binding of iron in this organism as compared with *Ectocarpus*.

Nature of the surface bound iron

Transmission Mössbauer spectroscopy (TMS) was utilized to determine more precise details of the surface iron and its surrounding ligands. The TMS spectra of a sample of *Macrocystis* grown for 19 days exposed to 3 μM ^{57}Fe-EDTA and not washed with the Ti reagent can be seen in Fig. 10.

The data can be fit with two doublets exhibiting the parameters shown in Table 1. The main component (species 1) has parameters which are typical for polymeric Fe(III) octahedrally coordinated to primarily oxygen ligands and fit into the range
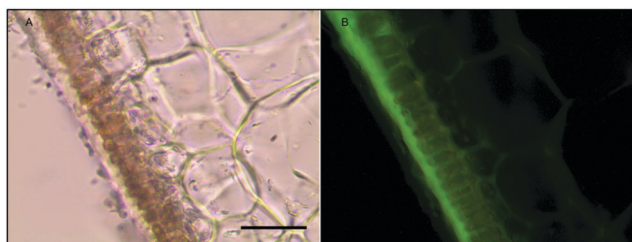

Fig. 6 Fe-MPNBD fluorescence of environmental sample of immature *Macrocystis* blade. (A) Brightfield transmission image. (B) Green fluorescence on the tissue surface and apoplast represent Fe-MPNBD complexation in areas with high concentrations of iron. Scalebar, 20 μm.
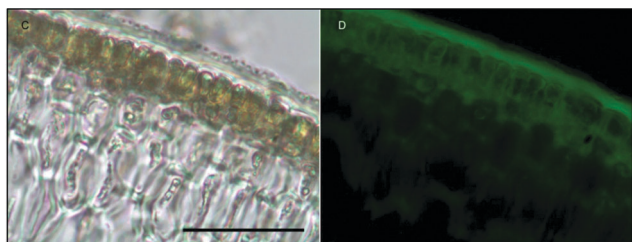

Fig. 7 Fe-MPNBD fluorescence of environmental sample of *Macrocystis* stipe meristoderm. (C) Brightfield transmission image. (D) Green fluorescence on the tissue surface and apoplast represent Fe-MPNBD complexation in areas with high concentrations of iron. Scalebar, 20 μm.
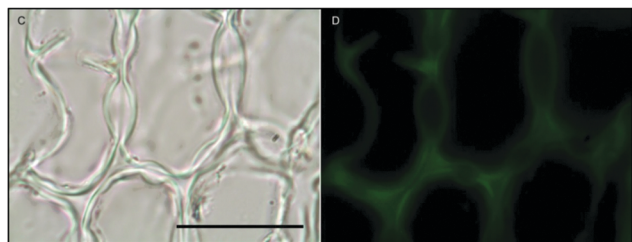

Fig. 8 Fe-MPNBD fluorescence of environmental sample of *Macrocystis* stipe cortex. (C) Brightfield transmission image. (D) Green fluorescence in the apoplast represent Fe-MPNBD complexation in areas with high concentrations of iron. Scalebar, 40 μm.
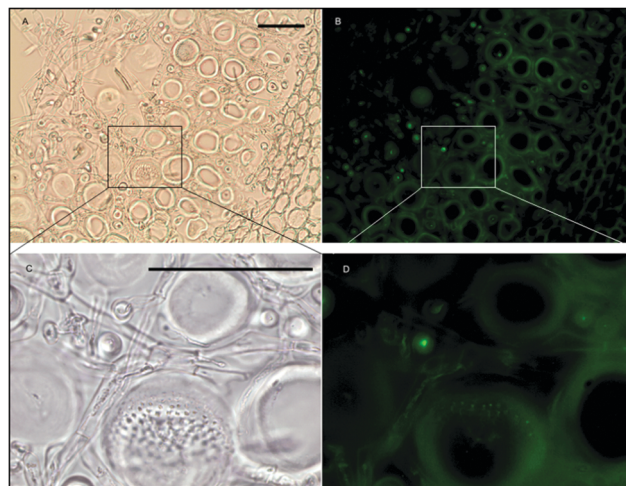

Fig. 9 Fe-MPNBD fluorescence of environmental sample of *Macrocystis* stipe medulla. (A) Brightfield transmission image. (B) Green fluorescence in the apoplast represent Fe-MPNBD complexation in areas with high concentrations of iron. (C) Brightfield transmission image. (D) Green fluorescence in the hyphae cell and sieve pores represent Fe-MPNBD complexation in areas with high concentrations of iron. Scalebar, 40 μm.

observed for carboxylate Fe(III) model complexes.[23] The minor species (2) exhibits parameters consistent with an iron sulfur cluster as previously seen in *Ectocarpus*.[24]

Iron storage

Microscopic and spectroscopic studies focusing on iron storage are challenging for organisms that have evolved efficient iron uptake strategies and consequently store little of this element. *Macrocystis* is one such organism with internal iron concentrations below the detection limit of light microscopy, and EDS. Thus, in this study methodology is limited to transmission Mössbauer spectroscopy (TMS). After long-term (19 days) incubation in ^{57}Fe-EDTA enriched culture medium and then washed with the Ti reagent to eliminate the surface bound iron, TMS spectra exhibiting sufficient resonance absorption were obtained which display a single quadrupole doublet-like feature (Fig. 11). Since the blade material was thoroughly washed with the Ti(III)–citrate–EDTA reagent, the presence of iron on the algal surfaces can be excluded and therefore, the iron components observed by TMS are genuinely of intracellular origin. From this, it can be concluded, that ^{57}Fe supplied as EDTA complex in the medium is transported into, and metabolized inside, cells of *Macrocystis*. A low percentage ($<0.2\%$) of the TMS signal experienced resonant absorption with the ^{57}Fe Mössbauer nucleus. A single iron compound detected by TMS displays a spectrum and parameters (Table 2) typical of a polymeric ($Fe^{3+}O_6$) system. Due to the weak signal at 77 K, low temperature TMS was below the detection limit, attributable to the doublet splitting into a sextet and an accompanying decrease in peak intensity when a polymeric iron species is present (data not shown). Polymeric biological ($Fe^{3+}O_6$) systems found by *in situ* Mossbauer spectra very often represent the mineral cores of ferritins. The Mössbauer spectroscopic features of such systems
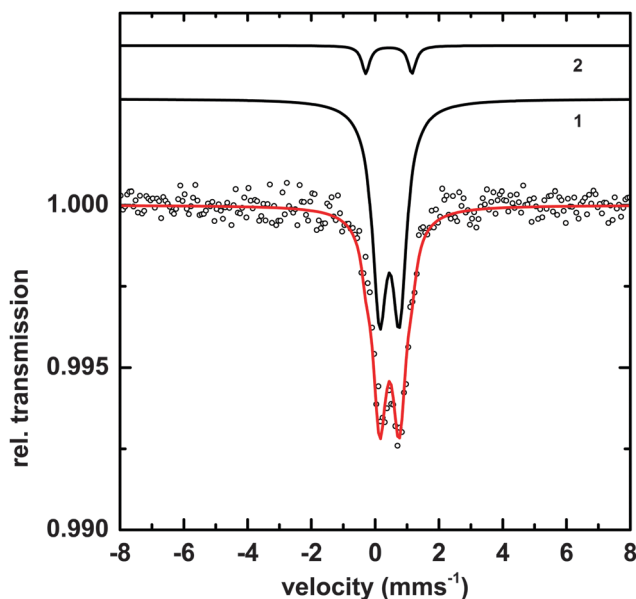
Fig. 10 TMS of *Macrocystis* blade after 19 day incubation in ^{57}Fe enriched growth medium. And not washed with the Ti–citrate reagent. Black circles indicated data points, species 1 and species 2 are separate components to the overall fit (red line).

Table 1 Mössbauer fit parameters of isomer shift (δ), quadrupole splitting (ΔE_Q), line width (Γ) and percentage of absorption area of *Macrocystis* blades not washed with Ti–citrate–EDTA at 77 K

Species		Parameter	Fitted value
1	$[Fe^{3+}O_6X_n^{\,m}]^{mn-9}$	δ	0.45 ± 0.01 mms^{-1}
		ΔE_Q	0.62 ± 0.02 mms^{-1}
		Γ	$0.\,55 \pm 0.02$ mms^{-1}
		Area	$93 \pm 1\%$
2	FeS	δ	0.43 ± 0.02 mms^{-1}
		ΔE_Q	1.45 ± 0.02 mms^{-1}
		Γ	0.30 ± 0.03 mms^{-1}
		Area	$7 \pm 1\%$

are strongly temperature and size dependent reflecting superparamagnetic relaxation of magnetic nanoparticles.[25] In lieu of an approximate blocking temperature, the relative degree of crystallinity and particle size of the mineral phase cannot be determined. However, based on the similarity of parameters with the TMS of *Ectocarpus*, it can be inferred that *Macrocystis* has a similar mineral core.

Discussion

Surface iron binding

Until recently, adsorption of iron to the cell surface of marine algae has been viewed as an experimental artifact complicating uptake studies. While it is indeed necessary to remove this signal when quantifying uptake, the potential biological significance of this surface bound iron has generally been ignored despite the fact that in some cases all the iron present in the media was in the form of the very stable Fe-EDTA chelate and
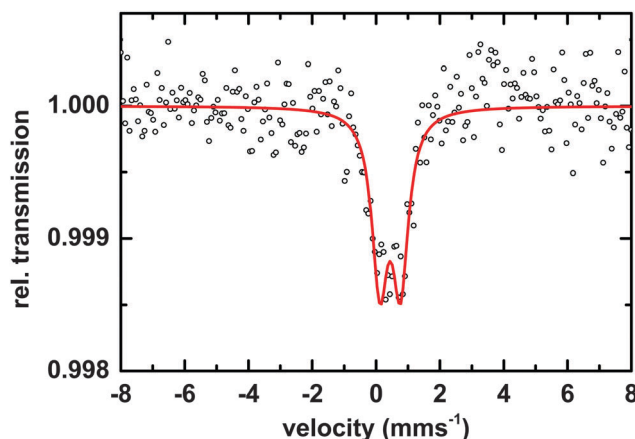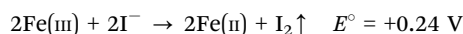

Fig. 11 TMS of *Macrocystis* blade grown for 19 days on 3 μM ^{57}Fe enriched culture medium after washing with Ti–citrate–EDTA reagent. Black circles represent data points and red line represents the fit to the data points.

Table 2 Mössbauer fit parameters of isomer shift (δ), quadrupole splitting (ΔE_Q), linewidth (Γ) and percentage of absorption area of *Macrocystis* blades after long term growth on ^{57}Fe (19 days) and washed with Ti–citrate–EDTA reagent measured at 77 K

Species		Parameter	Fitted value
$[Fe^{3+}O_6X_n^{\,m}]^{mn-9}$		δ	0.45 ± 0.01 mms^{-1}
		ΔE_Q	0.62 ± 0.02 mms^{-1}
		Γ	0.55 ± 0.03 mms^{-1}
		Area	100%

surface binding persisted even when an excess of EDTA was present. We have recently reexamined the extensive and powerful surface binding of iron found in filamentous brown alga *Ectocarpus siliculosus* and determined its effective binding constant, showed that the carboxylate groups from alginate were likely the biological ligands for iron and proposed a biological role for it.[12] It was expected that *Macrocystis* would behave similarly. However, the *Macrocystis* cell surface exhibits much weaker and less extensive iron-binding in comparison with *Ectocarpus*. This despite the fact that irrespective of the vastly different tissue morphologies of these two species, their cell walls are quite similar on a molecular level with alginate comprising 30–40% of the dry mass of both species.[26,27] It seems quite likely that in *Macrocystis* surface binding of iron is also *via* alginate carboxylate groups as alginase digestion eliminated nearly all of the surface bound iron and the effective binding constant was reduced by 6 orders of magnitude at pH 4. However the estimated effective surface binding constant, $\log K_{eff}'$ of around 18 at pH 8 is also significantly weaker than that for *Ectocarpus*. Histological staining and fluorescence of *Macrocystis* suggests iron is localized on the meristoderm surface in contact with seawater and also the apoplast of the meristoderm and cortex. Taken together, these results imply that from a standpoint of surface-bound iron as a function of biomass, it would appear that *Macrocystis* binds much less iron than *Ectocarpus* despite their similarity in cell wall composition. There are several possible explanations for this unexpected result.

One possibility is suggested by our preliminary results on the localization of both halide ions and iron. When we qualitatively examined the localization *via* EDS and histochemistry of both iron and (for an entirely different reason) iodine in *Macrocystis* blades from two different depths (0 m *i.e.* floating fronds and those found at 8 m) we found that at 8 m depth, the two elements are present at high enough concentrations to be observable by these techniques and are co-localized in the apoplast or cortical regions of the blade. In contrast, I and Fe concentrations on blades sampled from the surface both appear to be far less. Could the two events could be coupled to one another? Here cell surface bound Fe(III) could be envisioned to react (perhaps *via* a photochemically assisted pathway) with co-localized I$^-$ to produce I$_2$ and Fe(II) according to equation shown below to yield soluble Fe(II) and gaseous I$_2$ both of which can diffuse away into the water or atmosphere respectively and thus deplete their blade surface concentrations.

$$2Fe(III) + 2I^- \rightarrow 2Fe(II) + I_2\uparrow \quad E^\circ = +0.24\ V$$

Such a reaction between iodide and iron has recently been proposed to occur in a marine haptophyte and in terrestrial soils.[28,29]

Yet another possibility is suggested by the recent reports on the photoreactivity of Fe(III) alginate hydrogels where it was found that Fe(III) bound to alginate exposed to near UV light undergoes a photoreduction to Fe(II) with concomitant oxidative decarboxylation of the ligand reminiscent of the chemistry seen with some photoactive siderophores.[30] It therefore seems likely that any Fe(III) bound to the carboxylate groups of alginate on the surface of *Macrocystis* blades, some 85% of which float on the surface of the ocean and thus are exposed to strong sunlight, would also undergo this photochemistry. This would again result in formation of soluble Fe(II) which would then be lost to solution. Studies to see if this process might be important in a biological context are underway.

Internal iron storage

The vast majority of organisms store iron in one or more of the various forms of the ubiquitous protein ferritin. However, by genetic proximity to *Ectocarpus*, which clearly lacks homologs for ferritin in its genome the presence of ferritin in *Macrocystis* also seems unlikely. In the absence of ferritins two alternate or additional forms of iron storage have been identified in other organisms. The first, found in some fungi, is a siderophore based storage system clearly not present here.[31] The second, which has been elucidated in yeast and several other eukaryotes including the halotolerant alga *Dunaliella salina* is a vacuole based one.[32,33] At present there is little data in the literature about the chemical nature of vacuole sequestered iron stores. However it seems likely that the iron would be stored in some sort of mineral phase. Indeed it is reported that in *Arabidopsis* seeds some iron is located in vacuole globoids containing phytate which may bind ferric ions *via* phosphate groups.[34]

Since the spectroscopic parameters and relaxation properties (*i.e.* magnetic ordering temperatures) of condensed iron mineral phases are strongly dependent on particle sizes and their crystalline/amorphous structure, detailed temperature dependent Mössbauer measurements can shed light on the nature of any iron stores as we demonstrated for *Ectocarpus*. Unfortunately, the weak signal from *Macrocystis* hinders these measurements but nevertheless the TMS data we obtained from *Macrocystis* are consistent with storage of iron in a mineral phase similar to that found in *Ectocarpus*. Whether this mineral phase is crystalline or amorphous, phosphate rich or poor, and its the subcellular location remains to be determined. Work geared towards more fully characterizing this system using a focused synchrotron beam as a Mössbauer source is continuing.

Acknowledgements

References

1 P. R. Moog and W. Bruggemann, Iron reductase systems on the plant plasma-membrane – a review, *Plant Soil*, 1994, **165**, 241–260.
2 N. J. Robinson, C. M. Procter, E. L. Connolly and M. L. Guerinot, A ferric-chelate reductase for iron uptake from soils, *Nature*, 1999, **397**, 694–697.
3 V. Romheld and H. Marschner, Evidence for a specific uptake system for iron phytosiderophores in roots of grasses, *Plant Physiol.*, 1986, **80**, 175–180.
4 K. W. Bruland, J. R. Donat and D. A. Hutchins, Interactive influences of bioactive trace-metals on biological production in oceanic waters, *Limnol. Oceanogr.*, 1991, **36**, 1555–1577.
5 J. H. Martin and S. E. Fitzwater, Iron-deficiency limits phytoplankton growth in the Northeast Subarctic Pacific, *Nature*, 1988, **331**, 341–343.
6 D. A. Hutchins, W. X. Wang, M. A. Schmidt and N. S. Fisher, Dual-labeling techniques for trace metal biogeochemical investigations in aquatic plankton communities, *Aquat. Microb. Ecol.*, 1999, **19**, 129–138.
7 A. J. Milligan, C. E. Mioni and F. M. M. Morel, Response of cell surface pH to pCO$_2$ and iron limitation in the marine diatom Thalassiosira weissflogii, *Mar. Chem.*, 2009, **114**, 31–36.
8 A. Tovar-Sanchez, S. A. Sanudo-Wilhelmy, M. Garcia-Vargas, R. S. Weaver, L. C. Popels and D. A Hutchins, A trace metal clean reagent to remove surface-bound iron from marine phytoplankton, *Mar. Chem.*, 2003, **82**, 91–99.
9 R. J. M. Hudson and F. M. M. Morel, Distinguishing between extracellular and intracellular iron in marine phytoplankton, *Limnol. Oceanogr.*, 1989, **34**, 1113–1120.
10 R. Sutak, H. Botebol, P. L. Blaiseau, T. Leger, F. Y. Bouget, J. M. Camadro and E. Lesuisse, A comparative study of iron

uptake mechanisms in marine micro-algae: iron binding at the cell surface is a critical step, *Plant Physiol.*, 2012, **160**, 2271–2284.

11 R. Sutak, J. Slapeta, M. San Roman, J. M. Camadro and E. Lesuisse, Nonreductive Iron Uptake Mechanism in the Marine Alveolate Chromera velia, *Plant Physiol.*, 2010, **154**, 991–1000.

12 E. P. Miller, L. H. Böttger, A. J. Weerasinghe, A. L. Crumbliss, B. F. Matzanke, W. Meyer-Klaucke, F. C. Küpper and C. J. Carrano, Surface Bound Iron: A Metal Ion Buffer in the Marine Brown Alga Ectocarpus siliculosus?, *J. Exp. Bot.*, 2014, **65**, 585–594.

13 F. Frolow, A. J. Kalb and J. Yariv, Structure of a unique twofold symmetrical heme-binding site, *Nat. Struct. Biol.*, 1994, **1**, 453–460.

14 P. M. Harrison and T. H. Lilley, Ferritinin *Iron Carriers Iron Proteins*, ed. T. M. Loehr, VCH Publishers, New York, 1989, pp. 123–238.

15 B. F. Matzanke, Iron Storage in Microorganisms, in *Transition metals in microbial metabolism*, ed. G. Winkelmann and C. J. Carrano, Harwood Academic Publishers, Amsterdam, 1997.

16 S. L. Baldauf, The deep roots of eukaryotes, *Science*, 2003, **300**, 1703–1706.

17 B. Parker, Translocation in Giant Kelp *Macrocystis*: Rates, Direction, and Quantity of C14-Labeled Products and Fluorescein, *J. Phycol.*, 1965, **1**, 41–46.

18 R. Meguro, Y. Asano, S. Odagiri, C. Li, H. Iwatsuki and K. Shoumura, Nonheme-iron histochemistry for light and electron microscopy: a historical, theoretical and technical review, *Arch. Histol. Cytol.*, 2007, **70**, 1–19.

19 H. Roschzttardtz, G. Conéjéro, C. Curie and S. Mari, Identification of the Endodermal Vacuole as the Iron Storage Compartment in the Arabidopsis Embryo, *Plant Physiol.*, 2009, **151**, 1329–1338.

20 M. J. Park, H. S. Jung, Y. J. Kim, Y. J. Kwon, J. K. Lee and C. M. Park, High-sensitivity fluorescence imaging of iron in plant tissues, *Chem. Commun.*, 2014, **50**, 8547–8549.

21 S. L. Manley, Composition of Sieve Tube Sap from *Macrocystis* Pyrifera (phaeophyta) with Emphasis on the Inorganic Constituents, *J. Phycol.*, 1983, **19**, 118–121.

22 S. L. Manley, Micronutrient uptake and translocation by *Macrocystis* pyrifera (Phaeophyta), *J. Phycol.*, 1984, **20**, 192–201.

23 C. Dziobkowski, J. Wrobleski and D. Brown, Magnetic-Properties and Mossbauer-Spectra of Several Iron(III)-Dicarboxylic Acid Complexes, *Inorg. Chem.*, 1981, **20**, 671–678.

24 L. H. Böttger, E. P. Miller, C. Andresen, B. F. Matzanke, F. C. Küpper and C. J. Carrano, Atypical iron storage in marine brown algae: a multidisciplinary study of iron transport and storage in Ectocarpus siliculosus, *J. Exp. Bot.*, 2012, **63**, 5763–5772.

25 S. Mørup, *Magnetic Relaxation Phenomena*, Mössbauer Spectrosc. Transit. Met. Chem., Springer Berlin Heidelberg, 2011, pp. 201–234.

26 H. Takeda, F. Yoneyama, S. Kawai, W. Hashimoto and K. Murata, Bioethanol production from marine biomass alginate by metabolically engineered bacteria, *Energy Environ. Sci.*, 2011, **4**, 2575–2581.

27 G. Hernández-Carmona, D. J. McHugh, D. L. Arvizu-Higuera and Y. E. Rodríguez-Montesinos, Pilot plant scale extraction of alginates from *Macrocystis* pyrifera 4. Conversion of alginic acid to sodium alginate, drying and milling, *J. Appl. Phycol.*, 2002, **14**, 445–451.

28 S. A. van Bergeijk, L. Hernández-Javier, A. Heyland, M. Manchad and J. P. Cañavate, Uptake of iodide in the marine haptophyte Isochrysis sp. (T.ISO) driven by iodide oxidation, *J. Phycol.*, 2013, **49**, 640–647.

29 F. Keppler, R. Borchers, P. Elsner, I. Fahimi, J. Pracht and H. F. Schoeler, Formation of volatile iodinated alkanes in soil: results from laboratory studies, *Chemosphere*, 2003, **52**, 477–483.

30 G. E. Giammanco, C. T. Sonofsky and A. D. Ostrowski, Light Responsive Iron (III)-Polysaccharide Coordination Hydrogels for Controlled Delivery, *ACS Appl. Mater. Interfaces*, 2015, **7**, 3068–3076.

31 B. F. Matzanke, E. Bill, A. X. Trautwein and G. Winkelmann, Role of siderophores in iron storage in spores of Neurospora crassa and Aspergillus ochraceus, *J. Bacteriol.*, 1987, **169**, 5873–5876.

32 Y. Paz, E. Shimoni, M. Weiss and U. Pick, Effects of iron deficiency on iron binding and internalization into acidic vacuoles in Dunaliella salina, *Plant Physiol.*, 2007, **144**, 1407–1415.

33 E. Martinoia, M. Maeshima and H. E. Neuhaus, Vacuolar transporters and their essential role in plant metabolism, *J. Exp. Bot.*, 2007, **58**, 83–102.

34 V. Lanquar, F. Lelievre, S. Bolte, C. Hames, C. Alcon, D. Neumann, G. Vansuyt, C. Curie, A. Schroder A and U. Kramer, *et al.*, Mobilization of vacuolar iron by AtNRAMP3 and AtNRAMP4 is essential for seed germination on low iron, *EMBO J.*, 2005, **24**, 4041–4051.